Homogenization of Fickian and non-Fickian water diffusion in composites reinforced by hydrophobic long fibers: Application to the determination of transverse diffusivity

T. Peret, Alexandre Clément, Sylvain Fréour, Frédéric Jacquemin

Version of Record: https://www.sciencedirect.com/science/article/pii/S0263822319303058
Manuscript_fe98aa7684c42bf5c4c6ff9d5340b523

Homogenization of Fickian and non-Fickian water diffusion in composites reinforced by hydrophobic long fibers: application to the determination of transverse diffusivity

T. PERET[a,b], A. CLEMENT[b,*], S. FREOUR[b], F. JACQUEMIN[b]

[a] *Institut de Recherche Technologique Jules Verne, Chemin du Chaffault, 44340 Bouguenais, France*
[b] *Institut de Recherche en Génie Civil et Mécanique, UMR CNRS 6183, Université de Nantes, Centrale Nantes, 58 Rue Michel Ange, BP 420, 44606 Saint-Nazaire, France*

Abstract

The present paper investigates the water absorption by polymeric matrix composites at both microscopic (*i.e.* reinforcements are explicitly depicted) and macroscopic (*i.e.* homogeneous media) scales through a numerical homogenization method. In this work, the two linear diffusion Fick's and Langmuir's laws are considered. The effective transverse diffusivities of Uni-Directional laminates are computed with the help of the Finite Element Method and compared to both analytical models and experimental data. The impact of the distribution of the hydrophobic reinforcements within the matrix is also pointed out.

Keywords: composite materials, water diffusion models, transverse diffusivity, numerical homogenization, multiscale modeling.

1. Introduction

The use of glass or carbon fiber reinforced polymers (G/C FRP) spreads into many industrial sectors such as marine transports [1] and renewable marine energies [2]. The humid aging of such materials resulting from the immersion in the harsh marine environment may lead the structure to perform no longer its function. Among other benefits, from an engineering point of view, these heterogeneous materials are attractive because they can be tailored for each specific application. Nowadays, in order to perform fast design, the numerical studies are often performed considering the laminates as homogeneous materials. However, many macroscopic observations originate from micro-scale phenomena. One thus needs to take into account microscopic informations in order to properly reproduce the actual macroscopic behaviour through a Representative Volume Element (RVE) of the studied material. The water absorption by composite materials is a good example because reinforcements are often considered hydrophobic [3, 4, 5]. As a consequence, diffusion process only occurs inside the matrix phase. Unfortunately, limited computational means prevent designers

*Corresponding author :
alexandre.clement@univ-nantes.fr

from depicting each phase in macro-scale simulations. Therefore, the compromise between accuracy of the predictions and fast design makes the scale transition framework [6] a great candidate to obtain accurate physical properties without representing the microscopic geometrical details. Among all the available methods, the numerical homogenization is the one selected in this work. Numerical homogenization has been widely used to solve linear and non-linear mechanical [7, 8, 9] as well as thermal conduction [10, 11, 12] problems. However, the computation of diffusion effective properties, such as the transverse diffusivity of U.D. laminates, based on this approach has not been investigated. Analytical models have been yet proposed [3, 13, 14, 15] but only for fickian diffusion models.

The paper is organized as follows. Section 2 deals with the proposed modeling including the description of the studied domain, assumptions and diffusion constitutive equations. Then, Section 3 gives details concerning analytical and numerical computations of the transverse effective diffusivity. Section 4 presents the generator of realistic reinforcement distributions used in this work. Sections 5 and 6 are dedicated to the numerical investigations using the Finite Element Method. Two distinct studies are performed. The first application is dedicated to estimate the transverse diffusivity of U.D. laminate with respect to the volume fraction of reinforcements, in cases the polymer matrix satisfies the traditional Fick's law. All analytical, numerical and experimental results are confronted to each other. The second study deals with a non-Fickian matrix based composite. We compare the results between heterogeneous (on a single irregularly reinforced microstructure) and homogeneous representations according to local and global quantities of interest. Some concluding remarks are finally drawn in Section 7.

2. Modeling

2.1. Description of the studied domain

In this paper, both Equivalent Homogeneous Media (E.H.M) and heterogeneous materials are considered. They occupy the spatial domain $\Omega \in \mathbb{R}^d$ with $d \in \{1, 2, 3\}$ bounded by $\partial\Omega$. In the heterogeneous case $\Omega = \Omega_r \cup \Omega_m$, where Ω_m and Ω_r respectively represent the matrix and the reinforcements phases, as shown on figure 1.

[Figure 1 about here.]

For the homogeneous case, we simply write $\Omega = \Omega_{E.H.M.}$. The boundary $\partial\Omega$ is made up of two parts $\partial\Omega = \Gamma_c \cup \Gamma_j$. On Γ_c the moisture content corresponding to the environmental condition is set and on Γ_j the flux of water molecules is prescribed if needed. In the present work, all the material parameters are assumed constant at both spatial and time levels and independent of the results fields. On the other hand, the fibers are assumed hydrophobic and the diffusion problem will be therefore solely written on Ω_m for

the heterogeneous case. Polymeric resin constitutive of the matrix is considered as a homogeneous isotropic material. The resin is assumed perfectly healthy (*i.e.* without defects) and, particularly, porosity is not taken into account. From now on, the spatial average $\bar{\cdot}$, is defined by,

$$\bar{\cdot} = \frac{1}{mes(\Omega)} \int_{\Omega} \cdot \, d\Omega, \tag{1}$$

where $mes(\Omega)$ stands for the measure of the domain (*i.e.* length in 1.D., area in 2.D. and volume in 3.D.). In addition, macroscale quantities are also represented by over symbols or letters.

2.2. Diffusion problem

Usually, water diffusion problems involve the moisture content $c(\boldsymbol{x}, t)$, which, is defined at a material point of position $\boldsymbol{x}$ at time t by

$$c(\boldsymbol{x}, t) = \frac{m_w(\boldsymbol{x}, t)}{m_0(\boldsymbol{x})}, \tag{2}$$

where $m_w(\boldsymbol{x}, t)$ is the local water uptake, whereas $m_0(\boldsymbol{x})$ is the initial mass. However, for convenience and similarity with the heat conduction problem [13], we prefer to use the relative moisture content $r(\boldsymbol{x}, t)$ written as

$$r(\boldsymbol{x}, t) = \frac{c(\boldsymbol{x}, t)}{c^{\infty}(\boldsymbol{x})}, \tag{3}$$

where $c^{\infty}(\boldsymbol{x})$ is the maximum moisture absorption capacity of the considered phase. This property is determined experimentally and is given by the weight of a sample immersed in an environment of interest for a long period (weeks, months or even years depending on the material) divided by its initial weight. The spatial average relative moisture content $\overline{r}(t)$ on the domain Ω is computed from

$$\overline{r}(t) = \frac{1}{M_0} \int_{\Omega} \rho(\boldsymbol{x}) \, r(\boldsymbol{x}, t) \, d\Omega, \tag{4}$$

where $\rho(\boldsymbol{x})$ is the local density and M_0 denotes the initial sample mass. Afterwards, $\overline{r}(t)$ could also refer to the global relative moisture content.

2.2.1. The Fick's law

The Fick law [16, 17] is a common model to represent a diffusion process where each water molecule is free to move in the polymer network associated with domain Ω_m. Since the diffusivity D and the maximum moisture absorption capacity c^{∞} are assumed constant (*i.e.* independent of moisture content or mechanical states), the Fick local diffusion problem writes: find the solution field $r(\boldsymbol{x}, t)$ such that

$$\begin{aligned} \frac{\partial r}{\partial t} &= D\Delta r \quad \text{on } \Omega_m \times T, \\ r &= r_{imp} \quad \text{on } \Gamma_c \times T, \end{aligned} \tag{5}$$

where r_{imp} is the relative moisture content prescribed on Γ_c. From now, it will be set to 1.0. The latter comes from the fact that one would prescribed the maximum moisture capacity on Γ_c and, by definition,

$r_{imp} = \frac{c_{imp}}{c^\infty}$ which leads to a value of 1.0. For the Fick model, the water molecule flux $\phi_F(\boldsymbol{x}, t)$ is defined in this case by

$$\phi_F(\boldsymbol{x}, t) = -c^\infty \, D \, \nabla r(\boldsymbol{x}, t). \tag{6}$$

2.2.2. The Langmuir's law

Sometimes, experimental results exhibit water diffusion behaviors which do not follow the Fick's law as shown in [18, 19]: this might be called an anomaly of diffusion. For instance, in [20], the authors divided the water molecules diffusing through a single solid phase in two populations. The first, denoted $n(\boldsymbol{x}, t)$ is free to move while the molecules of the second phase, denoted $N(\boldsymbol{x}, t)$, are bonded to the polymer network due to reversible chemical reactions such as those occurring when moisture induced plasticization. A free water molecule could become a bonded one with a frequency α and, reciprocally, a bonded molecule could be freed with a frequency β. The total moisture content naturally verifies $c(\boldsymbol{x}, t) = n(\boldsymbol{x}, t) + N(\boldsymbol{x}, t)$. For a similar reason described in the Fick's law section, the relative fields $r_n(\boldsymbol{x}, t)$ and $r_N(\boldsymbol{x}, t)$ are being used from now on. Then, the Langmuir local diffusion problem writes: find the solution fields $r_n(\boldsymbol{x}, t)$ and $r_N(\boldsymbol{x}, t)$ such that they verify

$$\begin{array}{rcll} \frac{\partial r_n}{\partial t} + \frac{\partial r_N}{\partial t} & = & D\Delta r_n & \text{on } \Omega_m \times T, \\ \frac{\partial r_N}{\partial t} & = & \alpha \, r_n - \beta \, r_N & \text{on } \Omega_m \times T, \\ r_n & = & r_{n_{imp}} & \text{on } \Gamma_c \times T, \\ r_N & = & r_{N_{imp}} & \text{on } \Gamma_c \times T, \end{array} \tag{7}$$

where $r_{n_{imp}}$ and $r_{N_{imp}}$ are respectively the imposed free and bounded relative moisture content on Γ_c which naturally verify: $r_{n_{imp}} + r_{N_{imp}} = 1.0$. For this model, the water molecule flux $\phi_L(\boldsymbol{x}, t)$ is defined by

$$\phi_L(\boldsymbol{x}, t) = -c^\infty \, D \, \nabla r_n(\boldsymbol{x}, t). \tag{8}$$

Considering those two different populations, the Langmuir model is able to represent a wider class of diffusion phenomena the the Fick model. It is worth saying the latter is included in the former range.

3. Transverse diffusivity homogenization

Usually, the composite parts are often thin which, leads to neglect the in-plane water diffusion and only take into account the perpendicular or transverse diffusion. In this work, only the transverse diffusivity $D_\perp$ of U.D. laminates is investigated. However, a little remark about the diffusivity under fibers' direction could be stated. Assuming reinforcements are straight shaped, the water molecules' diffusion paths are parallel to the fibers, therefore the diffusion coefficient under the reinforcements direction must be equal to the resin's diffusivity [3]. As a result, the prediction of the longitudinal coefficient of diffusion in U.D. fiber-reinforced composites is not a critical issue, contrary to the case of the transverse coefficient of diffusion, which strongly depend on the volume fraction of matrix, for instance.

3.1. Analytical approach

The prediction of the transverse diffusivity of composite materials has been studied for a long time, since the pioneering works published by Shen and Springer in 1976 [3]. Most of the analytical models, developed in order to adress this issue, are based on either thermal conduction analogy [21] or on an electrical one [22]. A great synthesis work about those modelizations can be found in [23, 24]. The authors often assume a periodic distribution of the reinforcements within the matrix. In addition, in [13], thanks to the correspondence between the temperature and the relative moisture content and not the moisture content, the authors said the relations should be corrected by the following factor:

$$\kappa = \frac{1}{1 - v_r}, \tag{9}$$

where v_r is the volume fraction of reinforcements. Moreover, in [3], the authors assume the water molecules can only diffuse in a straight path squeezed between two columns of fibers. This latter leads to fictionally rise the volume fraction of reinforcements as shown on figure 2.

[Figure 2 about here.]

In order to make up this unrealistic hydrophobic part, it is necessary to modify the relation originally proposed in [3]. The table 1 presents the corrected analytical relations which provide the transverse diffusivity of U.D. composites $D_\perp$ divided by the matrix diffusivity D_m. All the curves of those ratios $D_\perp/D_m$ with respect to the volume fraction of reinforcements v_r are depicted on figure 3.

[Table 1 about here.]

As one may have expected, due to equivalent assumptions (regular distribution of the reinforcements, similarities between thermal and electrical conduction phenomena), the analytical models gave rather identical results unless for the very high values of $v_r > 65\,\%$ which are seldom reached in practice.

[Figure 3 about here.]

3.2. Numerical homogenization procedure

3.2.1. Maximum moisture absorption capacity

The water diffusion phenomenon is a peculiar case because of the definition of the relative moisture content $r(\boldsymbol{x}, t) = \frac{c(\boldsymbol{x},t)}{c^\infty}$, the maximum moisture absorption capacity is involved in the homogenization process and one needs to compute the macroscale maximum absorption capacity $\overline{c^\infty}$. In the case of hydrophobic reinforcements, the average moisture content $\overline{c}(t)$ is defined by

$$\overline{c}(t) = \frac{1}{\rho_m\, V_m + \rho_r\, V_r} \int_{\Omega_m} \rho_m\, c(\boldsymbol{x}, t)\, d\Omega_m, \tag{10}$$

where V_m, ρ_m, V_r and ρ_r respectively represent the volume or the density of the matrix and the reinforcements. When the permanent regime is reached, $\overline{c}(t)$ becomes $\overline{c^\infty}$ with

$$\overline{c^\infty} = \frac{\rho_m V_m}{\rho_m V_m + \rho_r V_r} c_m^\infty = \tau_m c_m^\infty, \tag{11}$$

where τ_m is the mass ratio of matrix within the laminate.

3.2.2. Fick diffusion model

The water diffusion problem according to the Fick's law is close to the thermal conduction with the Fourier's law. The latter has been strongly studied for a decade [8, 10, 12]. The sought effective property is the diffusivity tensor and more specifically coefficient $D_\perp$ which must verify the equality between the spatial average of the microscale water molecule flux $\overline{\boldsymbol{\phi}_F}(\boldsymbol{x})$ and the macro water molecule flux $\boldsymbol{\Phi}_F$ where those quantities are defined by

$$\overline{\boldsymbol{\phi}_F}(\boldsymbol{x}) = \frac{1}{mes(\Omega)} \int_\Omega \boldsymbol{\phi}_F \, d\Omega, \tag{12}$$

and

$$\boldsymbol{\Phi}_F = -\overline{c^\infty} D_\perp \overline{\nabla r}. \tag{13}$$

$\overline{\nabla r}$ is the gradient of relative moisture content at the macroscale. Therefore, to determine D, only a steady-state computation with specific boundary conditions imposed on $\partial\Omega$ is required. Using the more convenient periodic boundary conditions, the problem writes: find $r(\boldsymbol{x})$ such as

$$\begin{aligned} 0 &= D\Delta r_n && \text{on } \Omega, \\ r &= \overline{\nabla r}^0 \cdot \boldsymbol{x} + \tilde{r} && \text{on } \partial\Omega \end{aligned} \tag{14}$$

where $\overline{\nabla r}^0$ is a macroscopic uniform gradient of relative moisture content and $\tilde{r}$ is a periodic function over Ω. Periodic boundary conditions can be achieved through linear relationships between degrees of freedom. Many industrial finite element codes are provided with such feature. In this work, homogenization simulations were performed using code Aster [28].

3.2.3. Langmuir diffusion model

According to the water flux definition of the Langmuir's modelization 8, methodology used to compute the Fickian transverse diffusivity is efficient. However, one may also have a look at the two coefficients α and β involved in the exchange phase process modeled by

$$\frac{\partial r_N}{\partial t} = \alpha \, r_n - \beta \, r_N. \tag{15}$$

At the macroscopic scale, the above relation becomes,

$$\frac{\partial \overline{r_N}}{\partial t} = \overline{\alpha} \, \overline{r_n} - \overline{\beta} \, \overline{r_N}. \tag{16}$$

Furthermore,

$$\frac{\partial \overline{r_N}}{\partial t} = \overline{\frac{\partial r_N}{\partial t}} = \overline{\alpha}\,\overline{r_n} - \overline{\beta}\,\overline{r_N}, \tag{17}$$

and by definition of the spatial average,

$$\frac{\partial \overline{r_N}}{\partial t} = \frac{1}{mes(\Omega)} \int_\Omega \alpha(\boldsymbol{x})\, r_n(\boldsymbol{x},t)\, d\Omega - \frac{1}{mes(\Omega)} \int_\Omega \beta(\boldsymbol{x})\, r_N(\boldsymbol{x},t)\, d\Omega. \tag{18}$$

In glass or carbon reinforced polymer, it is common to consider reinforcements hydrophobic and this work and especially this section is no exception. In addition, assuming constant properties thus leads to

$$\frac{1}{mes(\Omega)} \int_\Omega \alpha(\boldsymbol{x})\, r_n(\boldsymbol{x},t)\, d\Omega = \alpha_m\, \overline{r_n(\boldsymbol{x},t)}, \tag{19}$$

and

$$\frac{1}{mes(\Omega)} \int_\Omega \beta(\boldsymbol{x})\, r_n(\boldsymbol{x},t)\, d\Omega = \beta_m\, \overline{r_N(\boldsymbol{x},t)}. \tag{20}$$

As a consequence,

$$\overline{\alpha} = \alpha_m \text{ and } \overline{\beta} = \beta_m. \tag{21}$$

In conclusion of this section, in this specific investigation of hydrophobic reinforcements laminates assuming constant properties, no additional developments are needed to perform homogenization in the case of the Langmuir's law. In this work, simulations involving Langmuir's law were performed using Abaqus [29] and a specific element developed under the UEL subroutine form as in [30]. The next section is devoted to the microstructure generator.

4. Generation of realistic microstructures

4.1. Experimental observations

In the previous section, the analytical relationships are based on a regular distribution of the reinforcements though it is an idealized representation. Indeed, figure 4 presents two images, taken with a Scanning Electron Microscope, one of a glass/polyester (left) and carbon/Epoxy (right) laminates. Add to the irregular reinforcements distributions, some highly and lowly densified areas are respectively emphasized by red and blue contours. Contrast had been emphasized by applying a filter to the photographies which allowed us to compute the volume fraction of reinforcements in the aforementioned areas : from 30 up to 40% in lowly densified areas and 65 up to 70% in highly densified ones.

[Figure 4 about here.]

Furthermore, one may notice that fibers are relatively circular; besides their diameter is almost constant. To enhance the numerical results, the reinforcement distributions accounted for achieving the computations should be as realistic as possible. These observations underline the interest of investigating both regular and irregular fiber distributions in numerical computations.

4.2. Numerical microstructure generator

In this section, the generator of microstructure geometries [37] is described. Based on the samples depicted on figure 4, the fibers are assumed perfectly circular with a unique diameter. Firstly, reinforcements are set regularly within the matrix. Secondly, fibers are provided with fictive speed vectors. Thirdly, as in a pool game, the distribution is progressively computed considering perfect elastic collisions. Finally, after a certain time or number of chocks, the microstructure is frozen. All those steps are synthesized on figure 5.

[Figure 5 about here.]

Thanks to this simple algorithm, dense (i.e. high volume fraction of reinforcements) quasi-realistic microstructures are quickly and easily produced.

5. Results

In this section, assuming a Fickian water diffusion behavior, the effective transverse diffusivities of U.D. laminates are computed. The F.E. software code Aster has been used to perform the simulations. The domain Ω is spatially discretized using bi-linear triangular elements. Due to the similarity between thermal conduction and Fick diffusion problems, we used linear thermal conduction elements available in the software's elements library. Furthermore, the number of elements has been scaled to ensure accurate numerical results. In the largest case, the mesh was composed of 250,000 elements.

5.1. Effective transverse diffusion coefficient

In order to compute the numerical curves of the ratio $D_\perp/D_m$, one must determine the size of the Representative Elementary Volume (R.E.V.) of the studied heterogeneous media. Commonly, to achieve this first step, effective properties are determined on increasingly larger Elementary Volume (E.V.) until convergence is reached. In this study, the size of the E.V. is represented by $\delta = \sqrt{n_r}$, where n_r is the number of fibers depicted in the E.V. The figure 6 presents the evolution of δ on regular microstructures. In the regular case, by using periodic boundary conditions the convergence is reached right away at $\delta = 1$.

[Figure 6 about here.]

Nevertheless, in irregular cases, the convergence may be so slow that it may not appear owing to machine limits. In [8, 31], the authors proposed to perform statistical studies on E.V. and to freeze the size when mean convergence is reached. In this work, statistical analyzes have been done through 100 computations and the volume fraction of reinforcements is set at $v_r = 60\,\%$. The figure 7 depicts the transverse diffusivity in the regular case $D_\perp^R$ in addition to both mean diffusivities along the two directions $D_\perp^X$ and $D_\perp^Y$ in irregular cases. No significant evolution is observed for E.V. of size greater than $\delta = 7$. In addition, $D_\perp^X$ and $D_\perp^Y$ are rather identical from that size which is kept as R.E.V. size in the following studies.

[Figure 7 about here.]

The higher dispersion in diffusivities observed on small E.V. is explained by the presence (or lack) of clusters of reinforcements within the domain. Besides, the lower the number of fibers, the more intense the effect of a cluster. In order to picture this phenomenon, an extreme case of a small E.V. ($\delta = 3$) is presented on figure 8. The reinforcement distribution clearly leads to a small diffusivity in the X direction whereas the diffusivity along the Y axis should be close to the matrix diffusivity. It is worth mentioning that the likelihood to produce such unbalanced reinforcements distribution decreases with the E.V. size.

[Figure 8 about here.]

5.2. Comparison with analytical and experimental results

The analytical and numerical results are plotted on figure 8. For the sake of clarity, legend symbols for analytical relations are identical to those used in figure 3 and numerical results are drawn in black. Naturally, regular distribution gives similar results than analytical modelizations. On the other hand, though irregular distributions curve shape is similar to the others, it is distinctly below. More precisely, the relative distance between regular (taken as reference) and irregular microstructures is $\epsilon = 15\%$.

[Figure 9 about here.]

Now, the impact of the type of microstructure on the computed effective transverse diffusivity has been highlighted but one might be interested to compare with experimental data. Since regular distribution and analytical models give close results, in order to keep plots as clear as possible, curves corresponding to analytical models have been removed. In [13], the authors synthesized pure resin and carbon/epoxy laminate experimental data. These experimental points and the computed diffusivity are presented on figure 10.

[Figure 10 about here.]

Actually, those experiments are tough for several reasons: pure resin could not be available, fabrication process for polymers and laminates are completely different, the volume fraction of reinforcements is not perfectly homogeneous, and side effects may appear. This is why, strong disparities in the experimental results for a given material may be observed. However, despite the significant variability of experimental data, one may carefully conclude that numerical computations over-estimate the transverse diffusivity, even in irregular cases. One could notice that the numerical diffusivity is 10 up to 40% higher than the experimental data at a volume fraction of reinforcement of $v_r = 60\%$. This gap rises even further as v_r increases. As v_r gets closer to 70% the numerical predictions become strongly erroneous (above 100%). Nevertheless, more experimental studies at high volume of reinforcements should be carried out in order to complete these results. Moreover, from a numerical point of view, models which take into account mechanical states in the diffusion phenomena, such as the one proposed in [32, 33, 34], are ought to be investigated.

6. Study of non-Fickian composites

Most studies about water diffusion in polymer based materials involved the Fick diffusion model. A practical explanation is due to its similarity with the thermal conduction problem. As a result, one can use thermal formulation of industrial F.E. codes, which is convenient [4, 5]. However, some materials exhibit non-Fickian water absorption behavior [19, 35] which is the subject of this section.

6.1. Presentation

The polymeric resin investigated in this section belongs to the epoxy family. The experimental results and the optimal fit (according to the least square criterion) are depicted on figure 11. The good correlation may be noticed. The diffusion phenomena in composites is often studied on specific coupons.

[Figure 11 about here.]

Those square specimen have small thickness over side length ratio $e/l << 1$. According to this geometry, water absorption by the edges can be neglected [3, 32]. Therefore, the diffusion problem becomes 2.D. so only the half top of the specimen is represented. The reinforcements are $7\,\mu m$ diameter carbon fibers and the volume fraction is set to $60\,\%$. In order to reach this high volume fraction, 950 fibers have been distributed using the generator described in section 4. Figure 12 shows the geometry of microstructure and the boundary condition used in simulations.

[Figure 12 about here.]

The environmental condition (in blue) is imposed on the top edge. The domain *Omega* is spatially discretized using bi-linear triangular elements. The number of elements, $240,000$ and $30,000$ respectively in heterogeneous and homogeneous cases, is large enough to ensure accurate results. On a 4 processors laptop, the computational time is approximately $2\,h$ for the heterogeneous case whereas it is a matter of minutes for the homogeneous domain. The table 2 presents all the properties used in the simulations at either microscopic or macroscopic scale.

[Table 2 about here.]

6.2. Local results

The local fields, for the relative content of free and bounded water molecules, for both heterogeneous and homogeneous cases, at two time steps (one transient t = 17 h and one close to steady-state t = 1055 h), are described on figure 13. Although the heterogeneous case iso-contours are not straight unlike in the homogeneous case, the local fields are consistent with each other but slight discrepancies might be noticed in the free water fields (figure 13 (a)) on the right part of the geometry where the moisture content is still very low.

[Figure 13 about here.]

Furthermore, it may be observed on figure 13, that both the matrix and the homogeneous media are saturated after an aging time of $1055\,h$. From fields depicted on figure 13, we propose the following diffusion scheme. First, free water molecules spread quickly within the resin, and then, chemical reactions with the polymer network chains occur. This behaviour may be related to the high diffusivity D compared to α and β.

6.3. Global results

The two absorption curves (average moisture content $\overline{c}$ over Ω at time t with respect to $\sqrt{t}$) are depicted on figure 14. At this scale the two simulations gave identical results, indicating that thanks to the homogenization method, heterogeneous and homogeneous diffusion computations using the Langmuir model are equivalent.

[Figure 14 about here.]

7. Conclusion

In this work, assuming constant properties, the effective transverse diffusivities of Uni-Directional laminates are determined within a numerical homogenization framework achieved owing to full-field approach. Furthermore, Fick and Langmuir laws are both studied. In addition, the impact of the reinforcements distribution on the macroscopic diffusivity has been highlighted. For this purpose, a microstructure generator, based on elastic chocks, has been used to create realistic fibers distribution according to S.E.M. photographies of glass/polyester and carbon/epoxy microstructures. Simulations were performed using the Finite Element Method. For the Langmuir model, a specific element (UEL) has been implemented in Abaqus. Two numerical studies were then achieved. In the first example we pointed out the effect of the fibers distribution within the matrix on the effective transverse diffusivity of U.D. laminates. This study puts the accent on the interest of using the irregular distributions which provide more representative results (according to the available experimental data) than the modeling based on regular microstructures. Secondly, heterogeneous and equivalent homogeneous simulation results have been compared. Both local and global quantities of a Langmuir based matrix composites were investigated. Very good agreements were obtained on fields of interests: moisture content, concentration of free and bound molecules between the two configurations. Although small differences appear at the microscale where the moisture content is very little, the sorption curves (*i.e.* macroscale) tell that the two media are equivalent. In order to pursue the present investigation, one should consider the possibility of modeling a coupling between the water diffusion physic and the mechanical state. In fact, in this work, the computed effective transverse diffusivities appear to be higher than literature experimental data and the latter leads to find a modeling which emphasizes the barrier effect of the hydrophobic reinforcements. Previous work on such couplings between mechanical

states and diffusion phenomena. For instance, works on the free volume theory have already been achieved but not in scale transition problems. Further works will be devoted to solve a micro-macro scale uncoupled hygro-mechanical problem by means of classical tools existing on linear elasticity and then investigate such diffusion-mechanical couplings in scale transition methods in order to take into account microscopic details at a higher scale like in multi-level (FE^2) computations.

8. Acknowledgements

This article is part of the ECOSAM2 project managed by IRT Jules Verne (French Institute in Research and Technology in Advanced Manufacturing Technologies for Composite, Metallic and Hybrid Structures). The authors wish to associate the industrial and academic partners of this project; respectively: ALSTOM, CETIM, DCNS and STX France.

References

[1] A. Mouritz, E. Geller, P. Burchill, K. Challis, Review of advanced composite structures for naval ships and submarines, Composite Structures 5 (2001) 21-41.

[2] D. Grogan, S. Leen, C. Kennedy, C. O Bradaigh, Design of composite tidal turbine blades, Renewable Energy 57 (2013) 151-162.

[3] C.-H. Shen, G. Springer, Moisture absorption and desorption of composite materials, Journal of Composite Materials 10 (1976) 2-20.

[4] P. Vaddadi, T. Nakamura, R. Singh, Transient hygrothermal stresses in fiber reinforced composites: a heterogeneous characterization approach, Composites: Part A 34 (2003) 719-730.

[5] Y. Joliff, L. Belec, M. Heman, J. Chailan, Experimental, analytical and numerical study of water diffusion in unidirectional composite materials - interphase impact, Computational Materials Science 64 (2012) 141-145.

[6] V. Nguyen, M.Stroeven, L.Sluys, Multiscale continuous and discontinuous modeling of heterogenous materials: A review on recent developments, Journal of Multiscale Modelling 3 (2011) 1-42.

[7] S. Hazanov, M. Amieur, On overall properties of elastic heterogeneous bodies smaller than the representative volume, International Journal of Engineering Science 33 (1995) 1289-1301.

[8] T. Kanit, S. Forest, I. Galliet, V. Mounoury, D. Jeulin, Determination of the size of the representative volume element for random composites: statistical and numerical approach, International Journal of Solids and Structures 40 (2003) 3647-3679.

[9] D. Francois, A. Pineau, A. Zaoui, Mechanical Behaviour of Materials, Volume 1: Micro- and Macroscopic Constitutive Behaviour, Springer, 2012

[10] M. Jiang, I. Jasiuk, M. Ostoja-Starzewski, Apparent thermal conductivity of periodic two-dimensional composites, Computational Material Science 25 (2002) 329-338.

[11] E. Monteiro, J. Yvonnet, Q. He, Computational homogenization for nonlinear conduction in heterogeneous material using model reduction, Computational Material Science 42 (2008) 704-712.

[12] I. Ozdemir, W. Brekelmans, M. Geers, Computational homogenization for heat conduction in heterogeneous solids, International Journal for Numerical Methods in Engineering 73 (2008) 185-204.

[13] K. Kondo, T. Taki, Moisture diffusivity of uni-directional composites, Journal of Composite Materials 16 (1982) 82-93.

[14] M. Woo, M. Piggott, Water absorption of resins and composites: Ivwater transport in fiber reinforced palstics, Journal of Composites, Technology and Research 10 (1988) 20-24.

[15] D. A. Bond, Moisture diffusion in a fiber-reinforced composite: Part-I - non-Fickian transport and the effect of fiber spatial distribution, Journal of Composite Materials 39 (2005) 2113-2129.

[16] A. Fick, On liquid diffusion, Philosophical Magazine and Journal of Science 10 (1855) 31-35.

[17] J. Crank, The mathematics of diffusion, 2^{nd} Edition, Oxford University Press, 1975.

[18] D. Perreux, D. Choqueuse, P. Davies, Anomalies in moisture absorption of glass fibre reinforced epoxy tubes, Composites: Part A 33 (2002) 147-154.

[19] S. Popineau, C. Rondeua-Mouro, C. Sulpice-Gaillet, M. E. Shanahan, Free/Bound water absorption inn an epoxy adhesive, Polymer 46 (2005) 10733-10740.

[20] H. Carter, K. Kibler, Langmuir-type model for anomalous moisutre diffusion in composite resins, Journal of Composite Materials 12 (1978) 118-131.

[21] G. Springer, S. Tsai, Thermal conductivities of unidirectional materials, Journal of Composite Materials 1 (1967) 166-173.

[22] L. Rayleigh, On the influence of obstacles arranged in rectangular order upon the properties of a medium, Philosophical Magazine 34 (1892) 481-502.

[23] L. Bao, A. Yee, Moisture diffusion and hygrothermal aging in bismaleimide matrix carbon fiber composites - part-I: Uni-weave composites, Composites Science and Technology 62 (2002) 2099-2110.

[24] H. Ramezani-Dana, A. Perronnet, S. Fréour, P. Casari, F. Jacquemin, Identification of moisture diffusion parameters in organix matrix composites, Journal of Composite Materials 47 (2013) 1081-1092.

[25] H. Kellert, D. Sachs, Calculations of the conductivity of a medium containing cylindrical inclusions, Journal of Applied Physics 35 (1964) 537-538.

[26] C. Shirell, J. Halpin, Moisture absorption and desorption in epoxy composite laminates, in: 4^{th} Conference on Composite Materials: Testing and Design, 1977.

[27] M. Piggott, Water absorption of resins and composites: Iv. water transport in fiber reinforced plastics, in: 6^{th} International Conference on Composite Materials and 2^{nd} European Conference on Composite Materials, 1987.

[28] Code Aster V12.5, EDF Group, 2015.

[29] Simulia, Abaqus Standard 6.12, Dassault System, 2012

[30] T. Peret, A. Clement, S. Freour, F. Jacquemin, Numerical transient hygro-elastic analyses of reinforced fickian and non-fickian polymers, Composite Structures 116 (2014) 395-403.

[31] W. Drugan, J. Willis, A micromechanics-based nonlocal constitutive equation and estimates of representative volume element size for elastic composites, Journal of the Mechanics and Physics of Solids 44 (1996) 497-524.

[32] S. Neumann, G. Marom, Prediction of moisture diffusion parameter in composite materials under stress, Journal of Composite Materials 6 (1987) 68-80.

[33] K. Derrien, P. Gilormini, The effect of applied stresses on the equilibrium moisture content in polymers, Scripta Materialia 56 (2006) 297-299.

[34] B.-E. Sar, S. Fréour, P. Davies, F. Jacquemin, Coupling moisture diffusion and internal mechanical states in polymers - a thermodynamical approach, European Journal of Mechanics A/Solids 36 (2012) 38-43.

[35] J. El Yagoubi, G. Lubineau, F. Roger, J. Verdu, A fully coupled diffusion-reaction scheme for moisture sorption-desorption in an anhydride-cured epoxy resin, Polymer 53 (2012) 5582-5595.

[36] D. Perreux, C. Suri, A study of the coupling between the phenomena of water absorption and damage in glass/epoxy composite pipes, Composites Science and Technology 57 (1997) 1403-1413.

[37] T. Peret, A. Clement, S. Freour, F. Jacquemin, Effect of mechanical states on water diffusion based on the free volume theory: Numerical study of polymers and laminates used in marine application, Composites: Part B 118 (2017) 54-66.

	$D_\perp/D_m$
A_1 [3]	$\frac{4}{\kappa\,(4-v_r^2\,\pi)}$
A_2 [22, 25]	$\kappa\,\frac{1-v_r-0.3058\,v_r^4}{1+v_r-0.3058\,v_r^4}$
A_3 [26]	$\kappa\,\frac{1-v_r}{1+v_r}$
A_4 [14, 27]	$\kappa\left(\frac{2}{\sqrt{1-\frac{4\,v_r}{\pi}}}\,tan^{-1}\sqrt{\frac{1+2\sqrt{v_r/\pi}}{1-2\sqrt{v_r/\pi}}}-\frac{\pi}{2+1-2\sqrt{v_r/\pi}}\right)$

Table 1: Analytical relations, extracted from literature, predicting the transverse diffusivity of U.D. composites scaled by matrix diffusivity.

	Epoxy	Carbon	Homogeneous
$\rho\ (kg/m^3)$	1310	1780	1592
$D\ (\mu m^2/s)$	2.04	–	0.992
$c^\infty\ (\%)$	1.71	–	0.5564
$\alpha\ (10^8\, s^{-1})$	7.17	–	7.17
$\beta\ (10^8\, s^{-1})$	7.45	–	7.45

Table 2: Properties for the microscopic constituents and the homogeneous media.

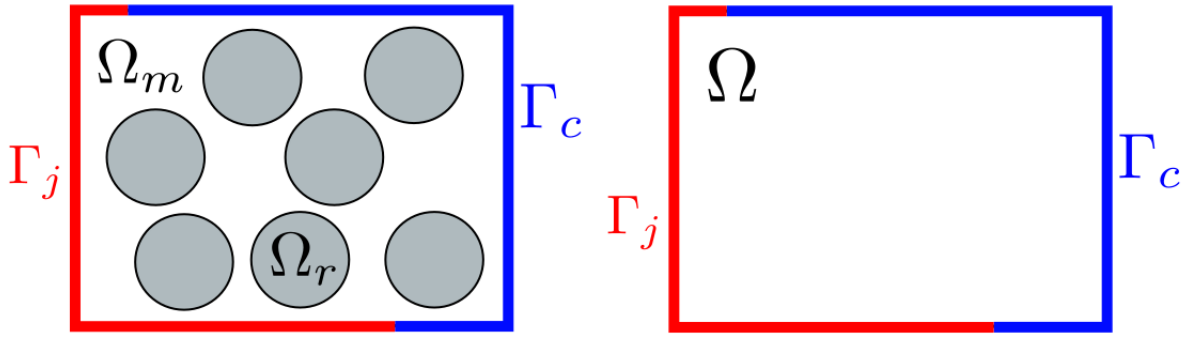

Figure 1: Heterogeneous and Equivalent Homogeneous Domains.

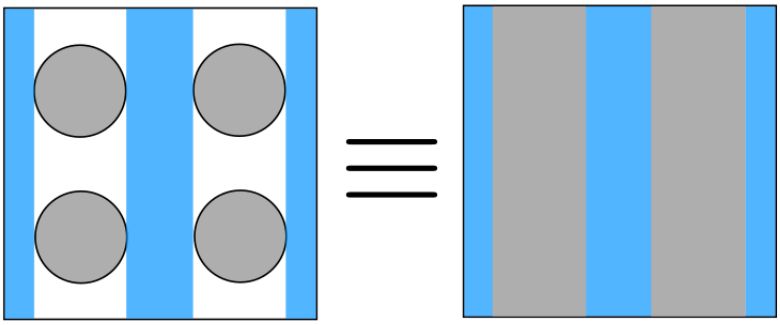

Figure 2: Representation of the water diffusion path according to [3].

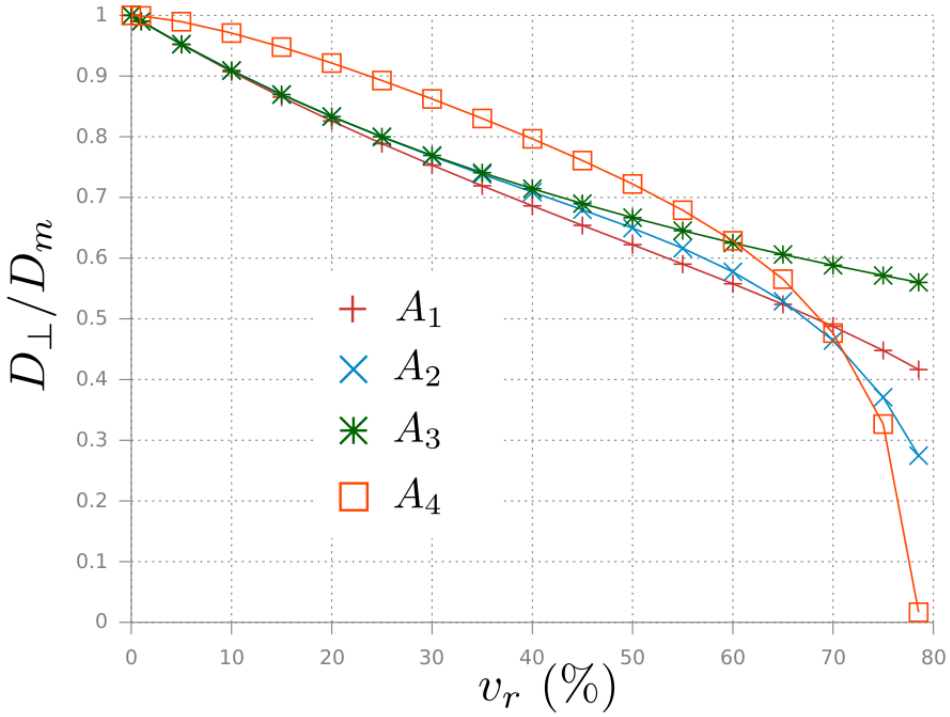

Figure 3: Curves of $D_\perp/D_m$ with respect to v_r for the analytical relations: A1 [3], A2 [22, 25], A3 [26], A4 [14, 27].

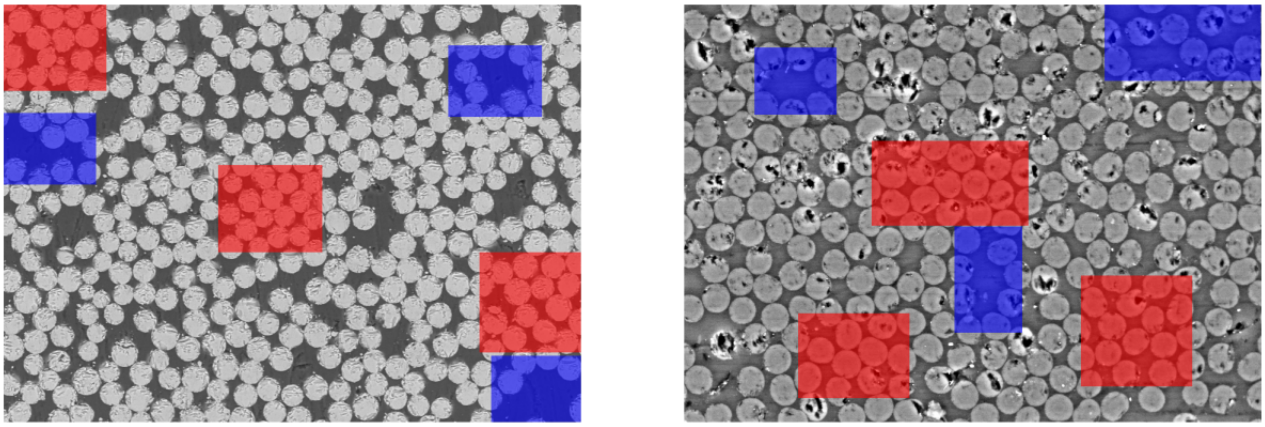

Figure 4: S.E.M. images of glass/polyester (left) and carbon/epoxy (right) microstructures.

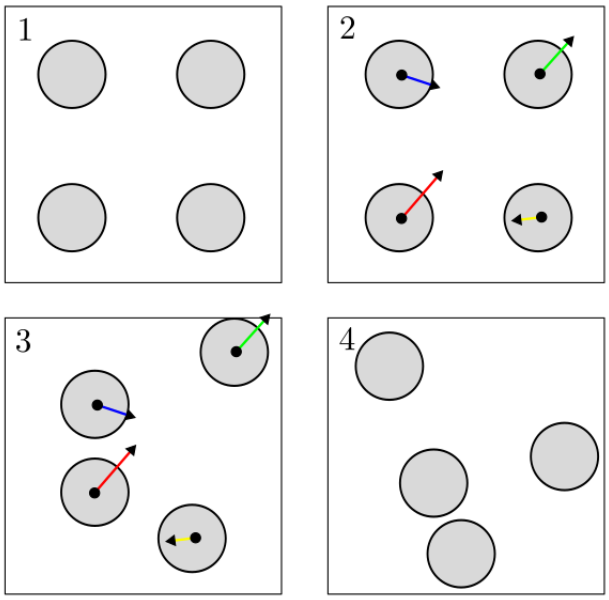

Figure 5: Steps of the microstructure generator [37].

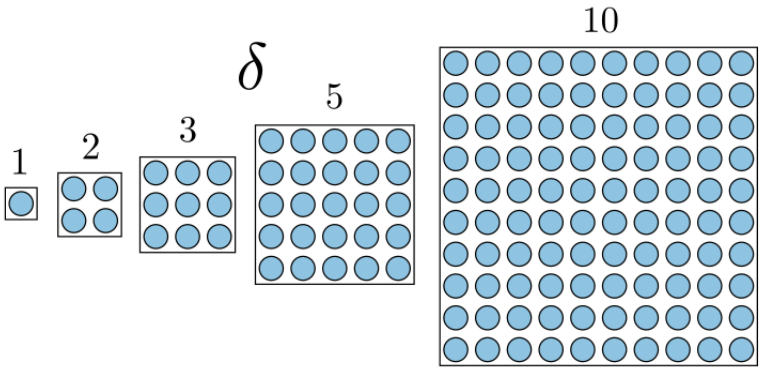

Figure 6: Evolution of the E.V. size according to parameter δ.

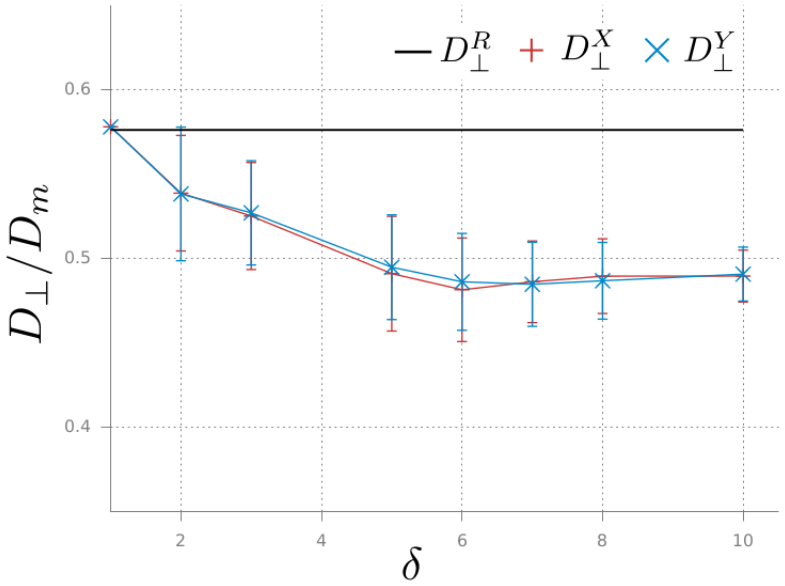

Figure 7: Convergence of the transverse diffusivity $D_\perp$ with respect to the E.V. size represented by δ.

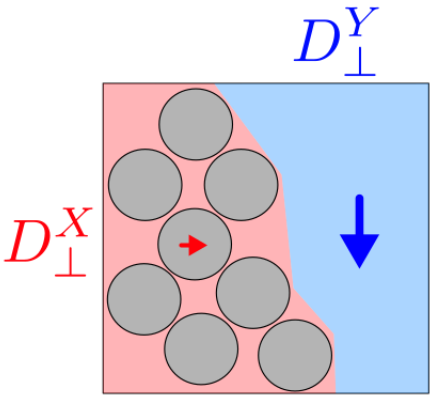

Figure 8: Example of the impact of clustering in a small E.V. $\delta = 3$.

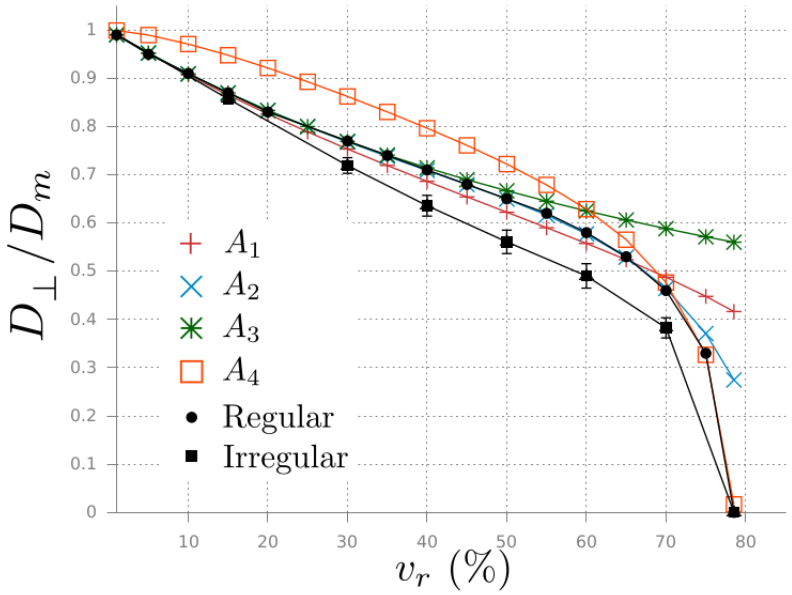

Figure 9: $D_\perp/D_m$ with respect to the volume fraction of reinforcements v_r. Comparison between analytical models and numerical results.

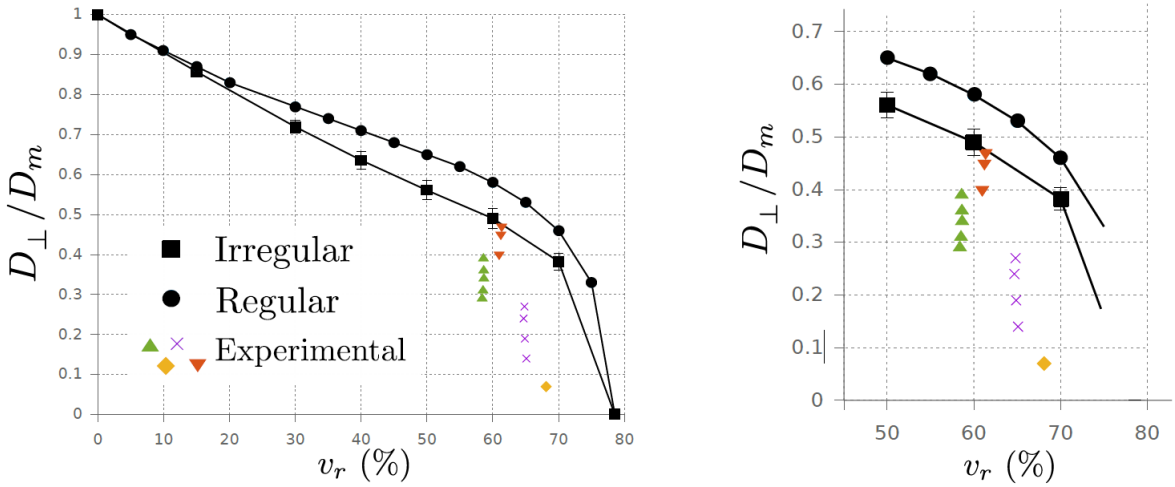

Figure 10: Comparison of experimental transverse diffusivities of carbon/epoxy laminates and numerical results (left). Zoom in on the interesting zone $50\,\% < v_r < 70\,\%$ (right).

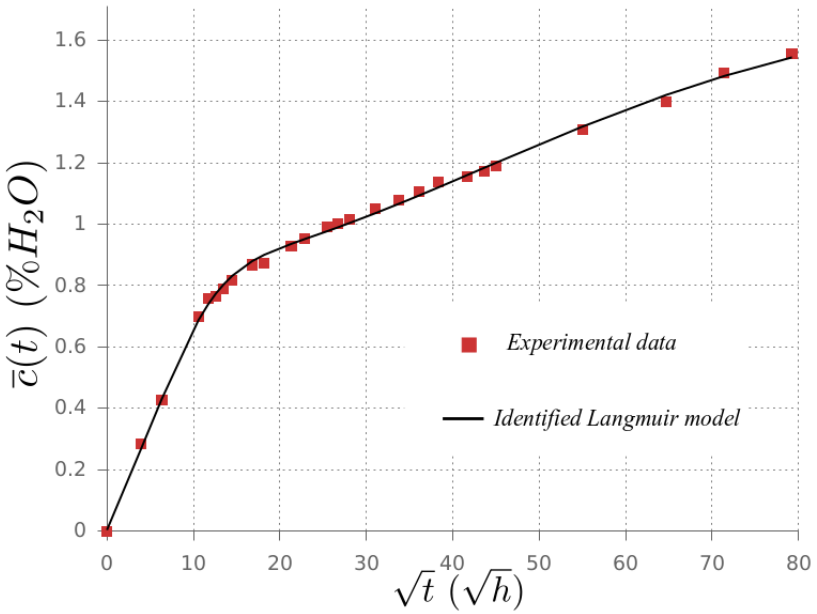

Figure 11: Anomalous water absorption behavior of an epoxy resin [36].

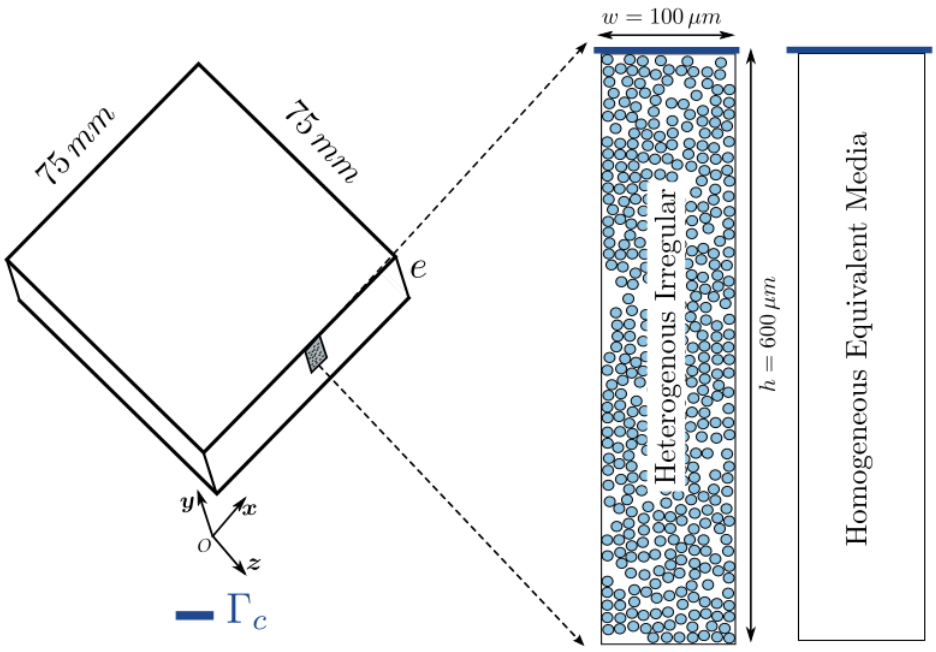

Figure 12: Geometries with the boundary condition used in computations.

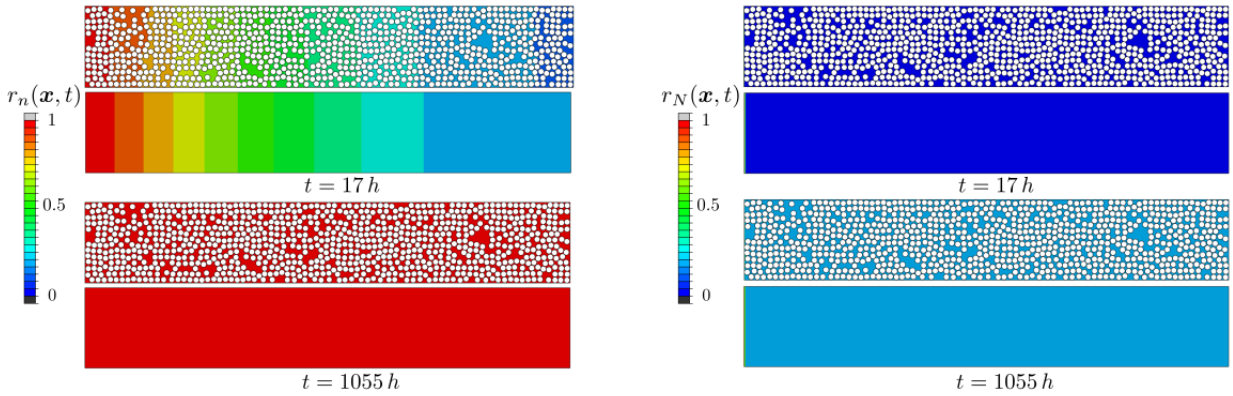

(a) (b)

Figure 13: Free (a) and bounded (b) water molecules fields at two transient times $t = 17\,h$ and $t = 1055\,h$ for both heterogeneous and homogeneous cases.

Figure 14: Macroscopic diffusion kinetics predicted owing to either the heterogeneous or homogeneous Langmuir models.